Pyroclastic currents and deposits: observation and impact

ISTITUTO NAZIONALE
DI GEOFISICA E VULCANOLOGIA

INGV
Sezione di Napoli

Dr. Domenico M. Doronzo
Osservatorio Vesuviano – INGV, Naples, Italy
domenico.doronzo@ingv.it

Lecture: ICELAND SUMMER SCHOOL 2021 – EUROVOLC

natural PC

experimental PC

a common approach with other currents??

sand and dust storm

snow avalanche

dusty current

natural PCs

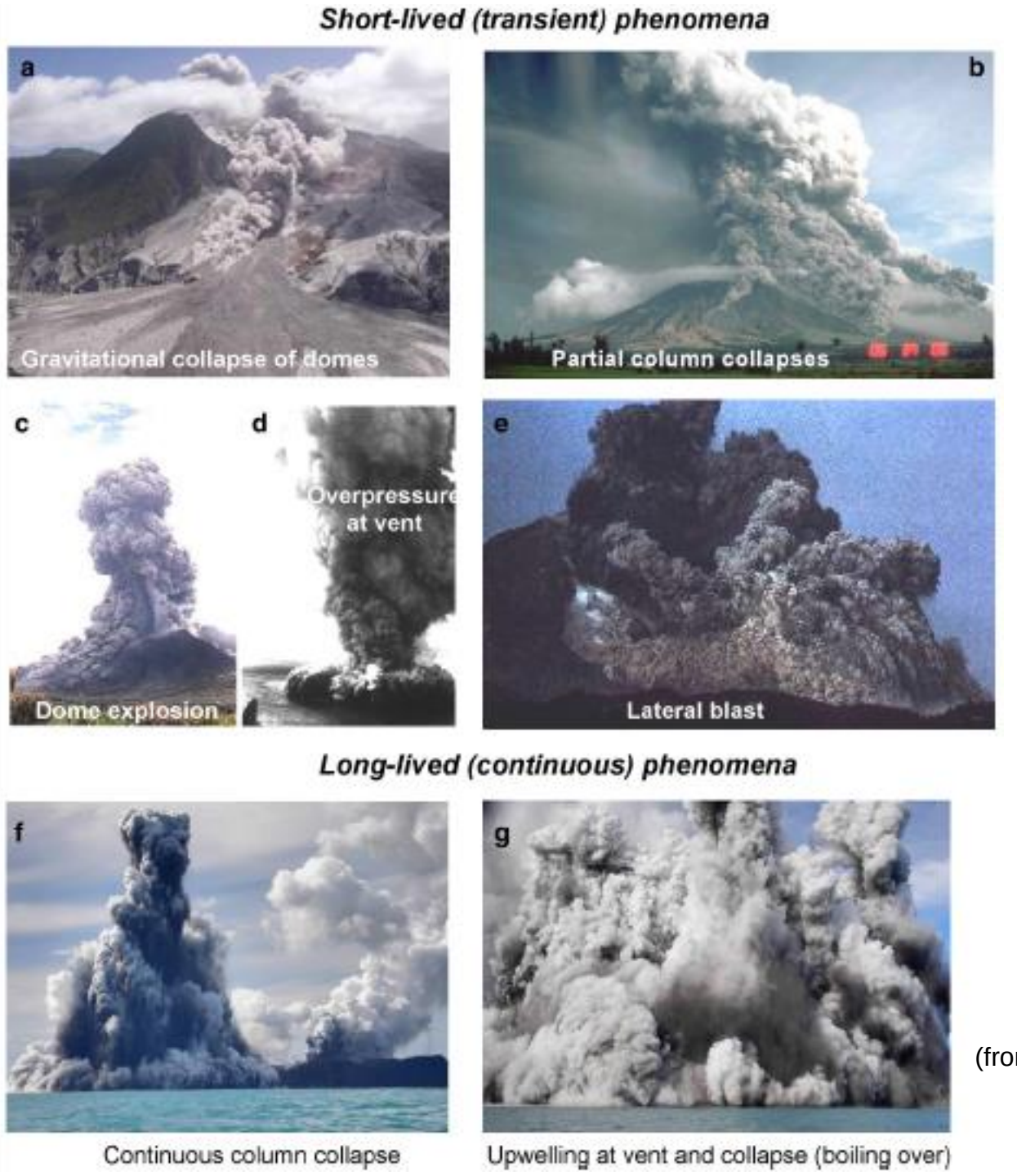

(from Sulpizio et al. 2014, JVGR invited review)

Structure of the lecture into three main sections + impact section:

1) EXPLOSION

2) TRANSPORT

3) DEPOSITION

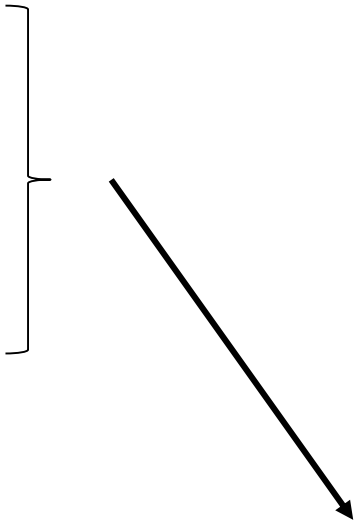

4) IMPACT

1) EXPLOSION

- Pyroclastic density currents (PCs) and their deposits are inevitably influenced by topography in explosive volcanism, but also depend on eruption style and duration (Giordano and Doronzo 2017, Sci. Rep.)

- Modelling, experiments and field deposits are used to understand the interaction between PDCs and **topography**, lithofacies associations, and eruptive processes

- Topography can be any morphological surface passed by a PC during the **eruption**, from local to volcano scale

Reviews on such topic are by Doronzo and Dellino (2014), and Sulpizio et al. (2014)

Doronzo D.M., Dellino P. 2014. Pyroclastic density currents and local topography as seen with the conveyer model. JVGR 278-279, 25-39

Sulpizio R., Dellino P., Doronzo D.M., Sarocchi D. 2014. Pyroclastic density currents: state of the art and perspectives. JVGR 283, 36-65 (INVITED REVIEW)

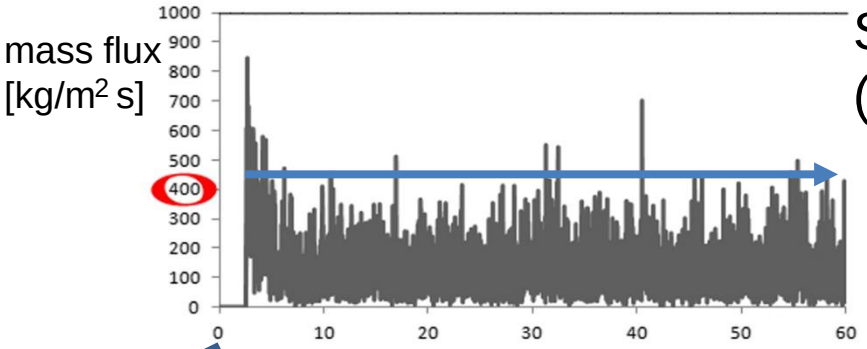

SUSTAINED FEEDING

($t_{supply}/t_{current} \geq 1$)

forced PC

(Doronzo 2012, JVGR; Giordano and Doronzo 2017, Sci. Rep.; Doronzo et al. in press, Terra Nova)

EXPLOSIVE ERUPTION

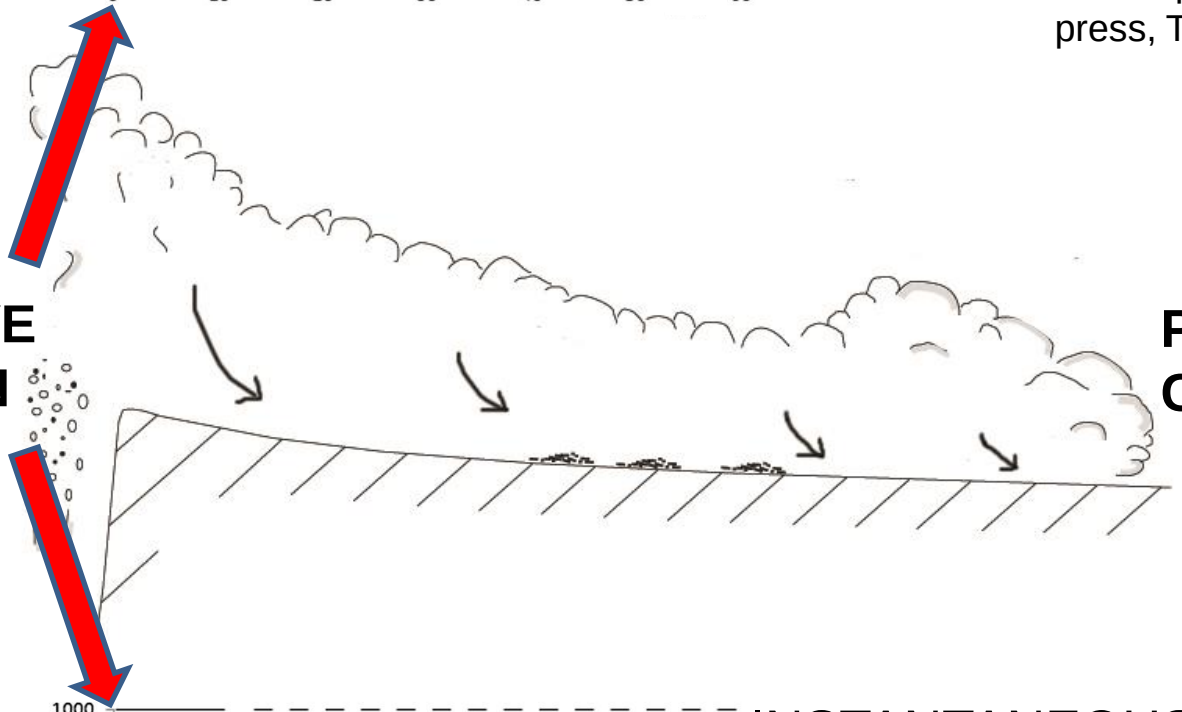

PYROCLASTIC CURRENT

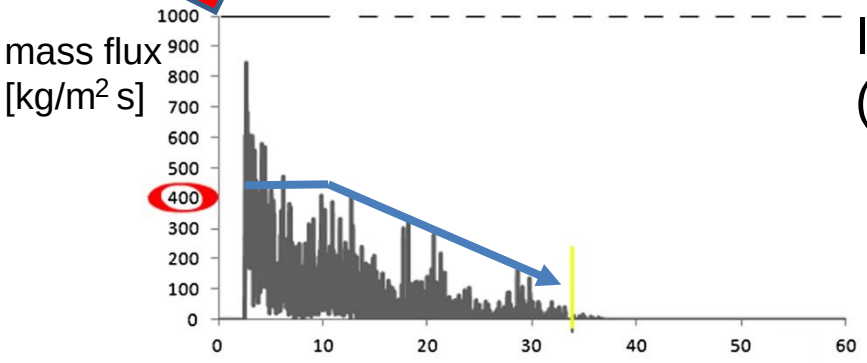

INSTANTANEOUS FEEDING

($t_{supply}/t_{current} < 1$)

inertial PC

(Doronzo 2012, JVGR; Giordano and Doronzo 2017, Sci. Rep.; Doronzo et al. in press, Terra Nova)

PC formation in explosive volcanism

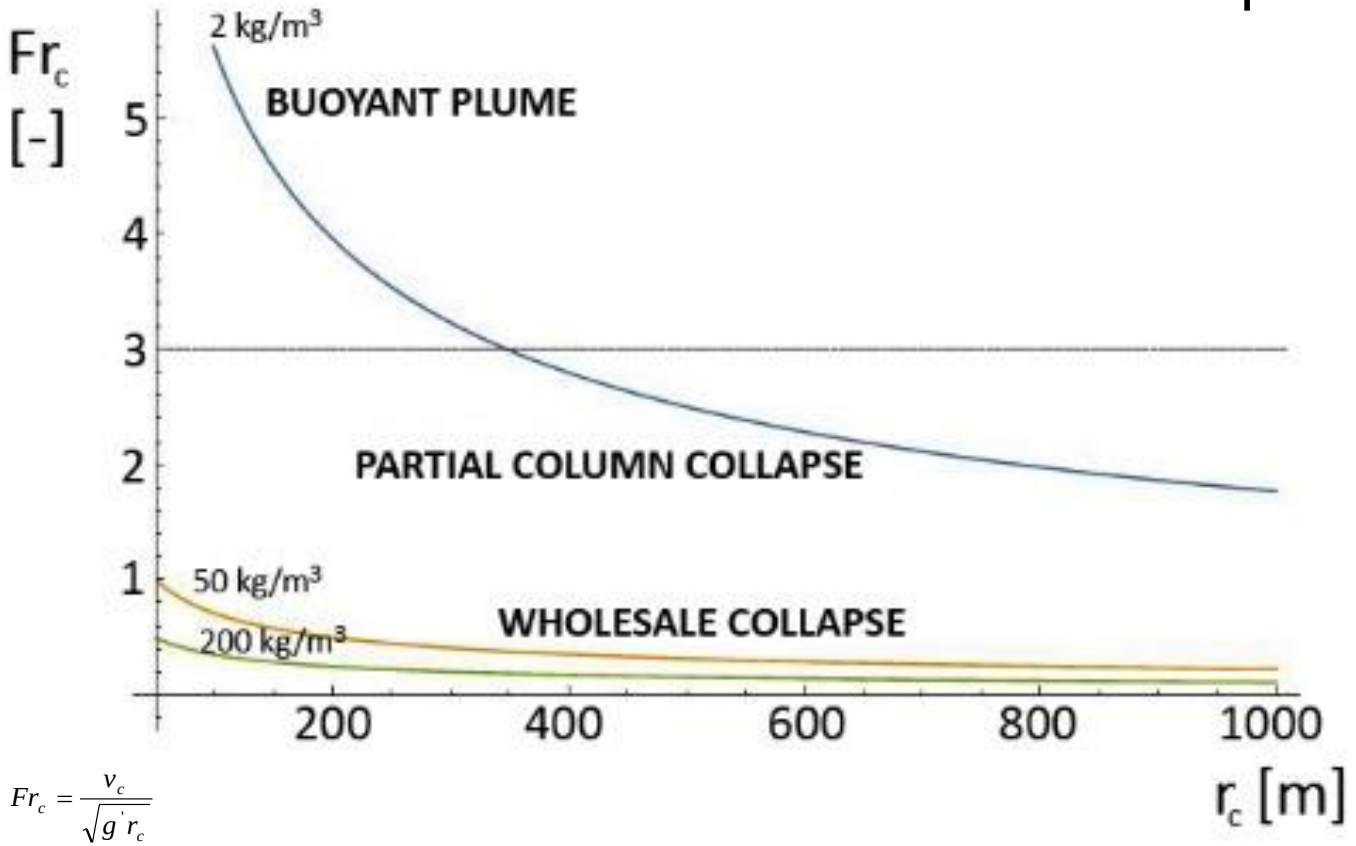

$$Fr_c = \frac{v_c}{\sqrt{g' r_c}}$$

$$g' = g\frac{\rho_c - \rho_a}{\rho_a}$$

$$\rho_c = \rho_p C_c + \sum_n \rho_n C_{nc}$$

$$\rho_p C_c = \sum_m \rho_m C_{mc}$$

$$\rho_c = \sum_m \rho_m C_{mc} + \sum_n \rho_n C_{nc}$$

structural and petrological conditions are responsible for PC formation

EXPLOSION – TRANSPORT – DEPOSITION scheme in geology (cf. turbidity currents)

Doronzo D.M., Giordano G., Palladino D.M. in press. *Energy facies*: A global view of pyroclastic currents from vent to deposit. Terra Nova, doi:10.1111/ter.12561

3D numerical simulation of large-scale experiments on PCs

The model is Eulerian-Lagrangian multiphase-type solving for primary gas phase, and secondary solid particles. The 3D Navier-Stokes + multispecies + turbulence + multiparticle equations are numerically solved using Ansys Fluent computational fluid dynamics platform

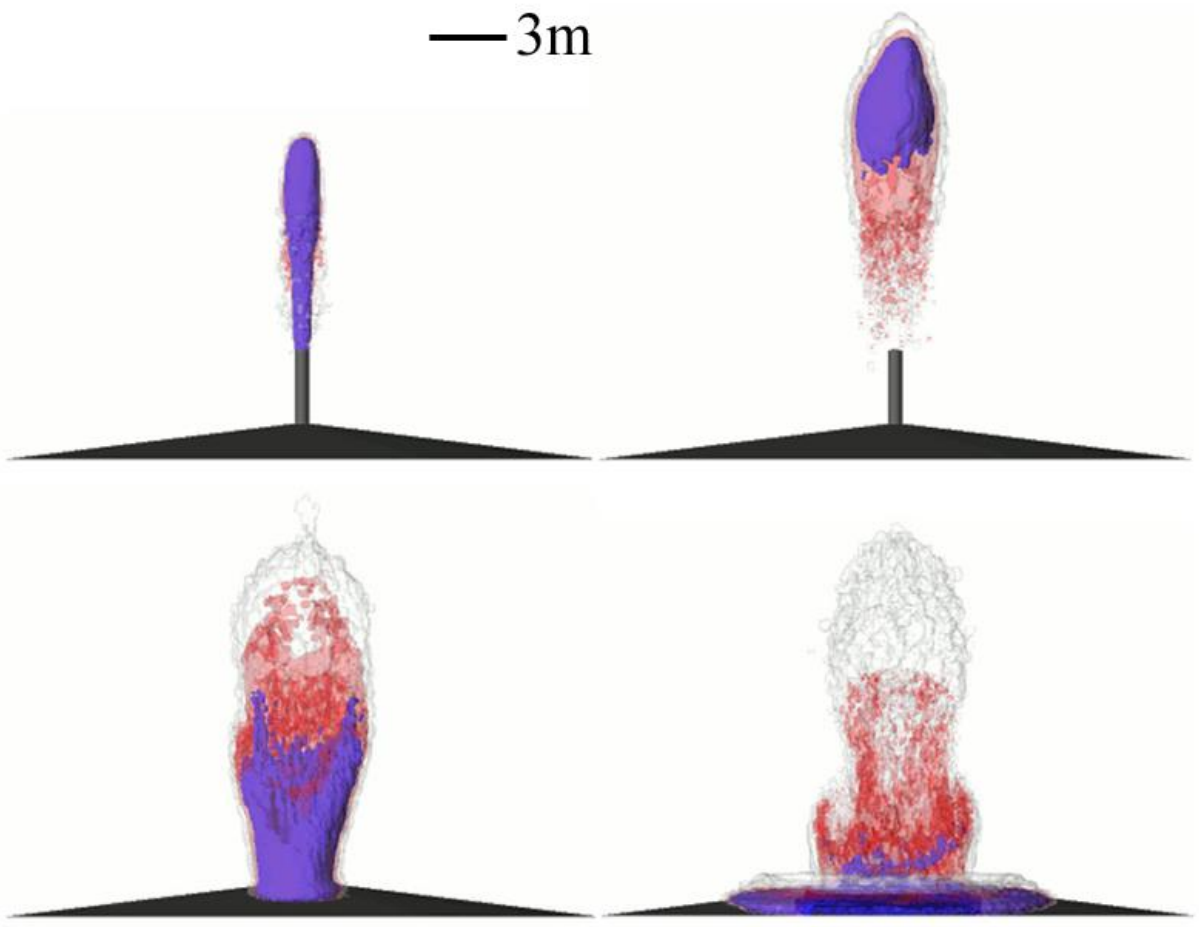

Contours of particle vol. concentration at 1s, 2s, 3s, and 4s of flow time

Doronzo D.M., de Tullio M.D., Dellino P., Pascazio G. 2011. Numerical simulation of pyroclastic density currents using locally refined Cartesian grids. Comp. Fluids 44, 56-67

test the utility and reliability of CFD for simulating pyroclastic flows.

We model the experiments by 3D unsteady Euler–Lagrange multiphase numerical simulations. As input data for the simulations the flow velocity, mass flow rate and grain size of the material at conduit exit were used, as described in the following sections.

3. Numerical scheme

3.1. An Euler–Lagrange multiphase approach to pyroclastic density currents

The gas–solid particle mixture of PDCs is modeled by an Euler–Lagrange multiphase approach, which treats the gas phase as a continuum and the particles as a discrete phase [2], exchanging mass, momentum, and energy with the fluid phase. The accuracy of such an approach is guaranteed for disperse flows of multiphase physics [8], and more generally for currents that have a particle volumetric concentration approximately up to 10–12% [2].

The turbulent flow field of the nitrogen-air mixture gas phase is computed solving the three-dimensional incompressible Reynolds Averaged Navier–Stokes (RANS) equations. Compressibility of the flow is neglected because the experimental flow velocity does not exceed 20 m/s and the energy equation is not solved since we consider cold experiments.

The time-averaged continuity and momentum equations are given in tensor notation and Cartesian coordinates by

$$\frac{\partial \bar{u}_j}{\partial x_j} = 0 \tag{1}$$

$$\frac{\partial}{\partial t}(\rho \bar{u}_i) + \frac{\partial}{\partial x_j}(\rho \bar{u}_i \bar{u}_j - \bar{\tau}_{ij}^{tot}) + \frac{\partial \bar{p}}{\partial x_i} - \rho g_i = 0 \tag{2}$$

where overbar indicates the generic variable (velocity components u_i and pressure p) averaged over a time interval that is large compared to the period of the random fluctuations associated with turbulence, but small with respect to the time variation of the flow field of unsteady flows. g is the gravity acceleration (9.81 m/s^2), and the density is implemented by a volume-weighted mixing law, between the densities of nitrogen (1.13 kg/m^3) and air (1.22 kg/m^3).

Since a nitrogen–air mixture is considered, a continuity equation for the conservation of the nitrogen and air is associated to the governing equations. It is given by

$$\frac{\partial}{\partial t}(\rho Y_n) + \frac{\partial}{\partial x_j}(\rho \bar{u}_j Y_n) = -\frac{\partial}{\partial x_j}(J_n) \tag{3}$$

where

$$J_n = -\left(\rho D_n + \frac{\mu_t}{Sc_t}\right)\frac{\partial}{\partial x_j}(Y_n) \tag{4}$$

$$\bar{\tau}_{ij}^{lam} = \mu\left(\frac{\partial \bar{u}_i}{\partial x_j} + \frac{\partial \bar{u}_j}{\partial x_i}\right) \tag{5}$$

$$\bar{\tau}_{ij}^{turb} = -\rho\overline{u_i' u_j'} \approx \mu_t\left(\frac{\partial \bar{u}_i}{\partial x_j} + \frac{\partial \bar{u}_j}{\partial x_i}\right) - \frac{2}{3}\rho k \delta_{ij} \tag{6}$$

$k = \frac{\overline{u_i' u_i'}}{2}$ being the turbulent kinetic energy, where u_i' is the fluctuating part of the velocity components,

$$\mu_t = \rho C_\mu \frac{k^2}{\varepsilon} \tag{7}$$

is the turbulent viscosity, δ_{ij} is the Kronecker delta, ε the turbulent dissipation rate and C_μ is an empirical constant equal to 0.0845 [29]. μ is the molecular viscosity, which is implemented by a mass-weighted mixing law, between the viscosities of nitrogen (1.66×10^{-5} kg/m s) and air (1.78×10^{-5} kg/m s).

In order to evaluate the turbulent viscosity, a turbulence model is required. In volcanology, two equation k–ε type turbulence models have been recently used when a RANS approach is employed to solve the PDC flow field [13,14,23,24,25]. These models have been validated both experimentally [11] and numerically [23] for their applications to the PDC physics. In particular, Dufek and Bergantz [23] performed, with success, several validation tests, by comparing their results with well-established direct numerical simulation results [34]. Here, the Re-normalization Group (RNG) k–ε model is used:

$$\frac{\partial}{\partial t}(\rho k) + \frac{\partial}{\partial x_j}(\rho \bar{u}_j k) = \frac{\partial}{\partial x_j}\left[\alpha_k(\mu + \mu_t)\frac{\partial k}{\partial x_j}\right] + \bar{\tau}_{ij}^{turb}\frac{\partial \bar{u}_i}{\partial x_j} - \rho\varepsilon \tag{8}$$

$$\frac{\partial}{\partial t}(\rho \varepsilon) + \frac{\partial}{\partial x_j}(\rho \bar{u}_j \varepsilon) = \frac{\partial}{\partial x_j}\left[\alpha_\varepsilon(\mu + \mu_t)\frac{\partial \varepsilon}{\partial x_j}\right] + C_{1\varepsilon}\frac{\varepsilon}{k}\bar{\tau}_{ij}^{turb}\frac{\partial \bar{u}_i}{\partial x_j} - C_{2\varepsilon}\rho\frac{\varepsilon^2}{k} - R_\varepsilon \tag{9}$$

The empirical constants α_k, α_ε, $C_{1\varepsilon}$ and $C_{2\varepsilon}$ are equal to 1.393, 1.393, 1.42, and 1.68, respectively [29]. The R_ε term is useful in the zones of the domain where the volcanic column impacts the ground surface and a high deformation rate of the fluid occurs and it is given by

$$R_\varepsilon = \frac{C_\mu \rho \eta^3 (1 - \eta/4.38)}{1 + 0.012\eta^3}\frac{\varepsilon^2}{k} \tag{10}$$

where

$$\eta \equiv \bar{S}k/\varepsilon \tag{11}$$

$$\bar{S} = (2\bar{S}_{ij}\bar{S}_{ij})^{1/2} \tag{12}$$

$$\bar{S}_{ij} = \frac{1}{2}\left(\frac{\partial \bar{u}_i}{\partial x_j} + \frac{\partial \bar{u}_j}{\partial x_i}\right) \tag{13}$$

In the context of the Euler–Lagrange approach, the fluid phase is treated as the continuum, whereas the solid particles are treated as the discrete phase and their individual trajectories are calculated inside the continuum on the basis of the fluid solution [2]. Similar applications are found on multiphase flows of Powder Technology

The model is Eulerian-Eulerian multiphase-type solving also for compressibility effects

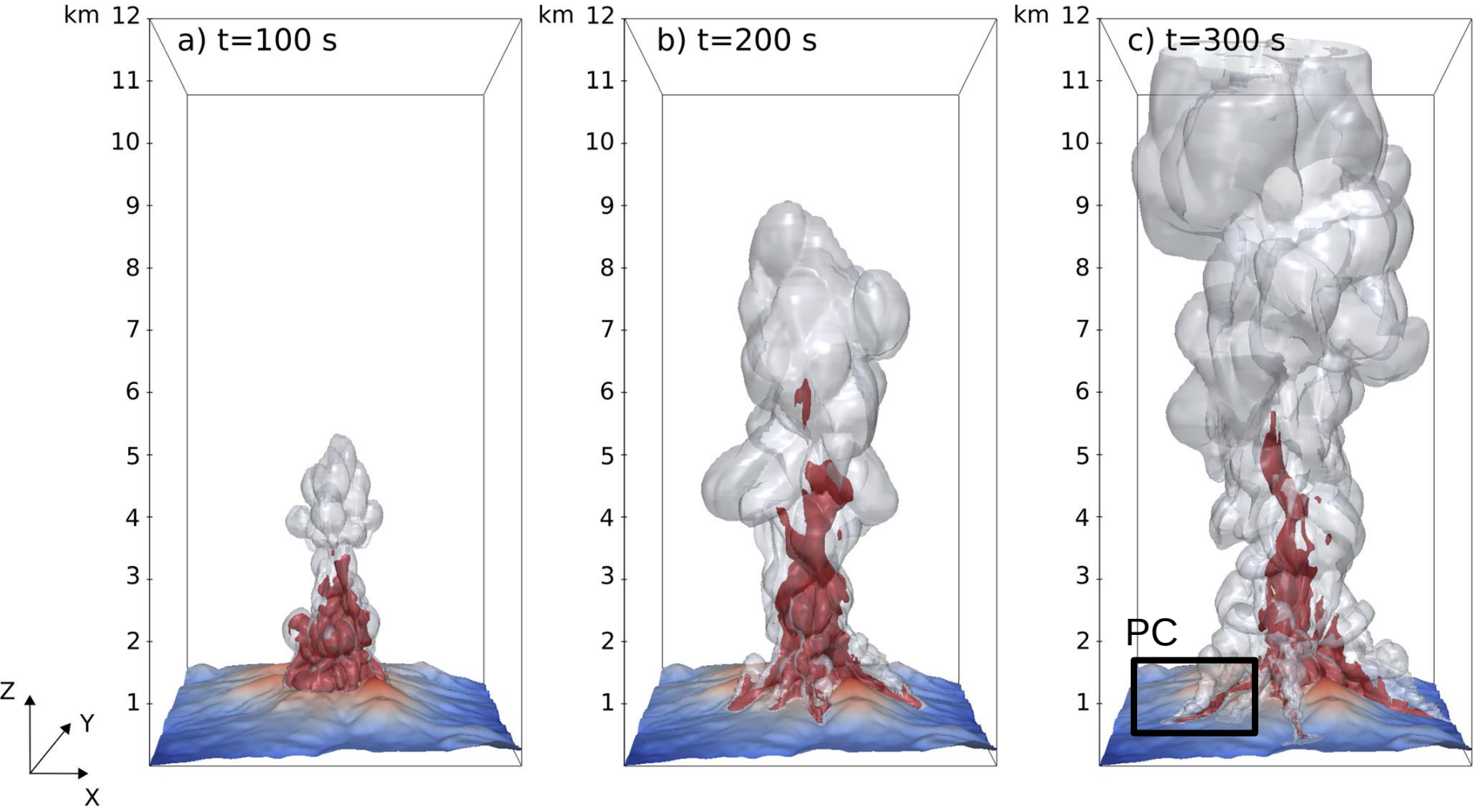

Esposti Ongaro T., Komorowski J.C., Legendre Y., Neri A. 2020. Modelling pyroclastic density currents from a subplinian eruption at La Soufrière de Guadeloupe (West Indies, France). Bull. Volcanol. 82, 76

Experiments are important in multiphase flow physics to calibrate theoretical and numerical models. Real volcanic material from Vesuvio, Campi Flegrei, Etna, and Vulture were used here to generate a conduit flow (post-fragmentation), and to reproduce Plinian and Vulcanian collapses versus buoyant plumes

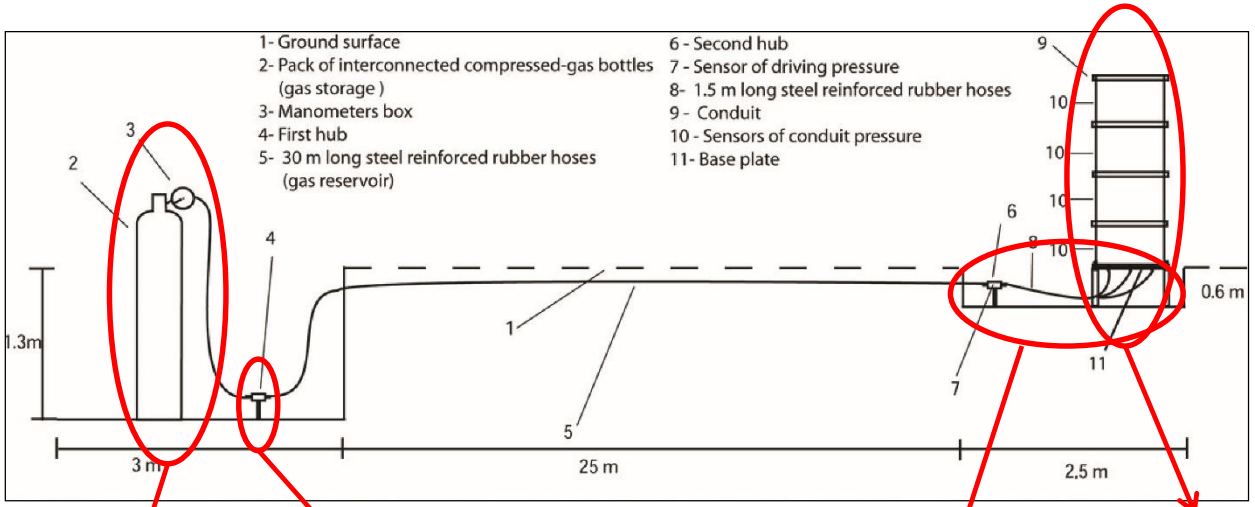

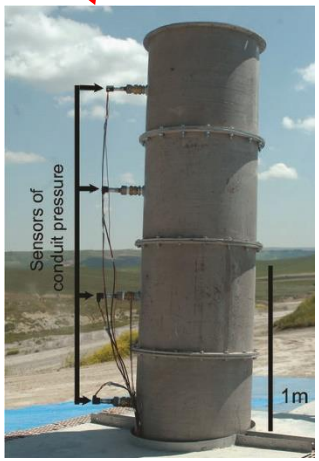

Dellino P. et al. 2010. Conduit flow experiments help constraining the regime of explosive eruptions. J. Geophys. Res. 115, B04204

vertical column and plume

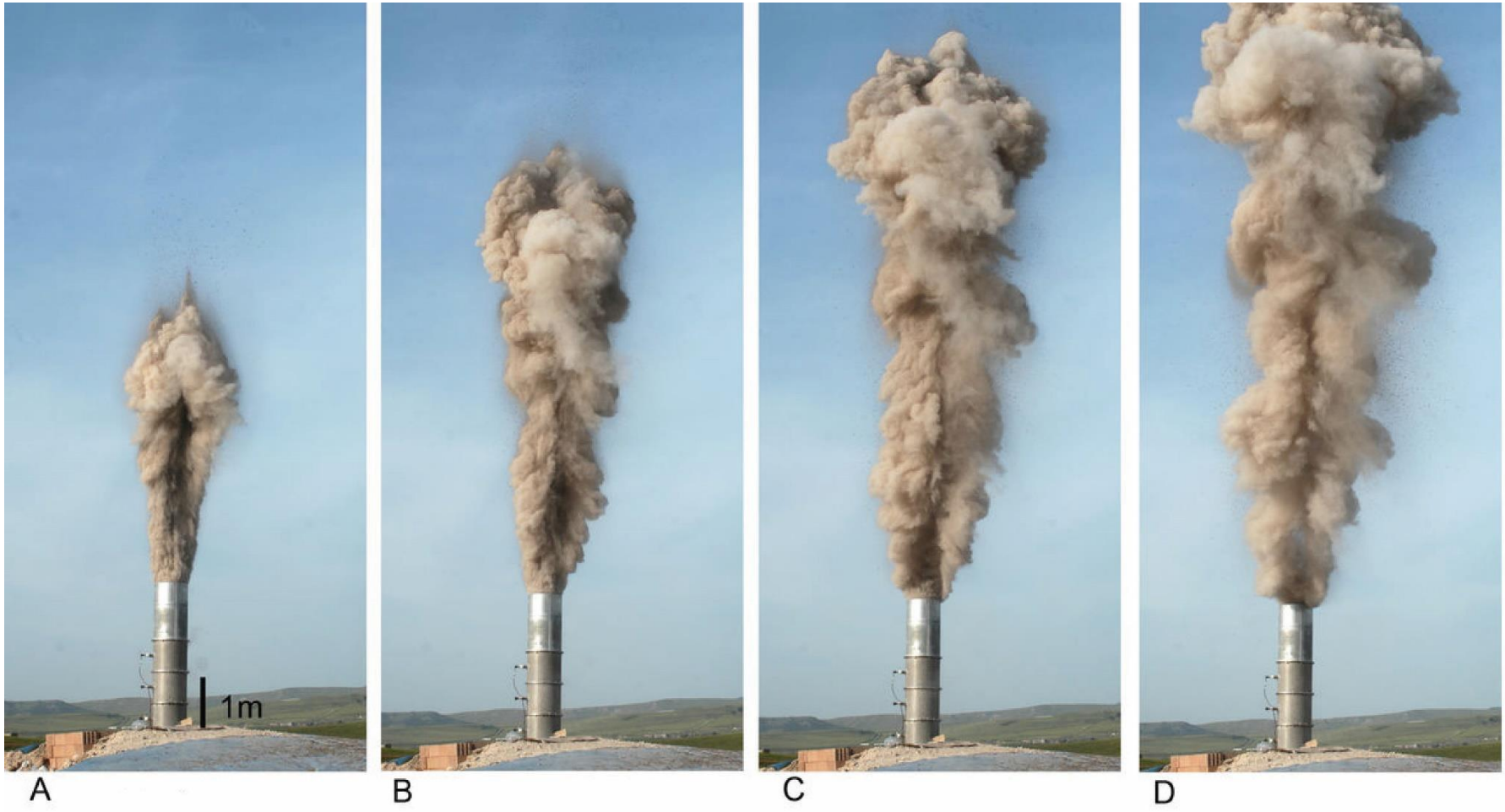

vertical column and collapse

A

B

C

D

overpressure expansion

A

B

C

D

2) TRANSPORT

Large-scale experiments are also important for detecting lateral flow structure (viscous sublayer, turbulent boundary layer, wake region)

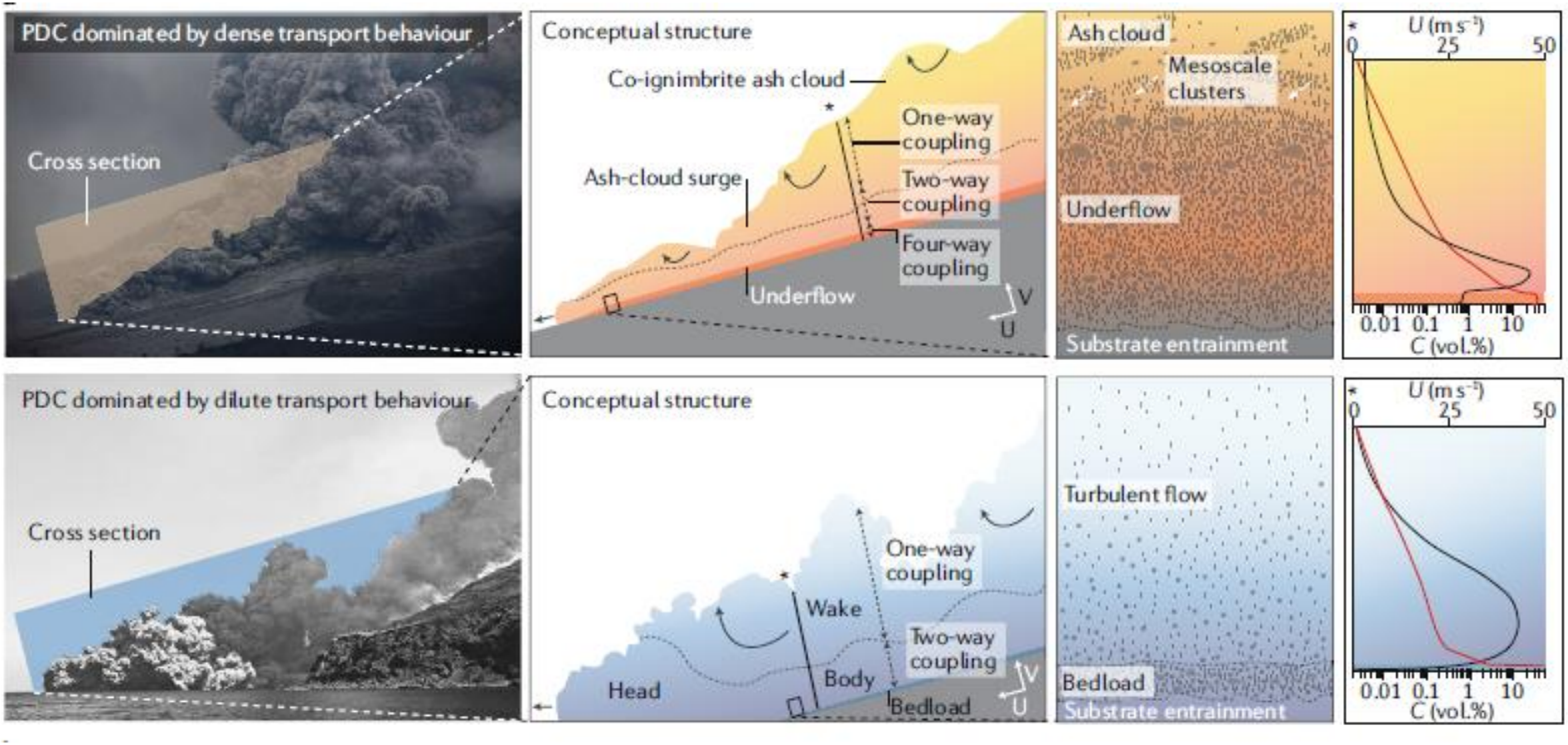

Lube G. et al. 2020. Multiphase flow behaviour and hazard prediction of pyroclastic density currents. Nat. Rev. Earth Environ. 1, 348-365

Fluidization experiments on the basal part of PC: transport and emplacement (aggradation to en-masse)

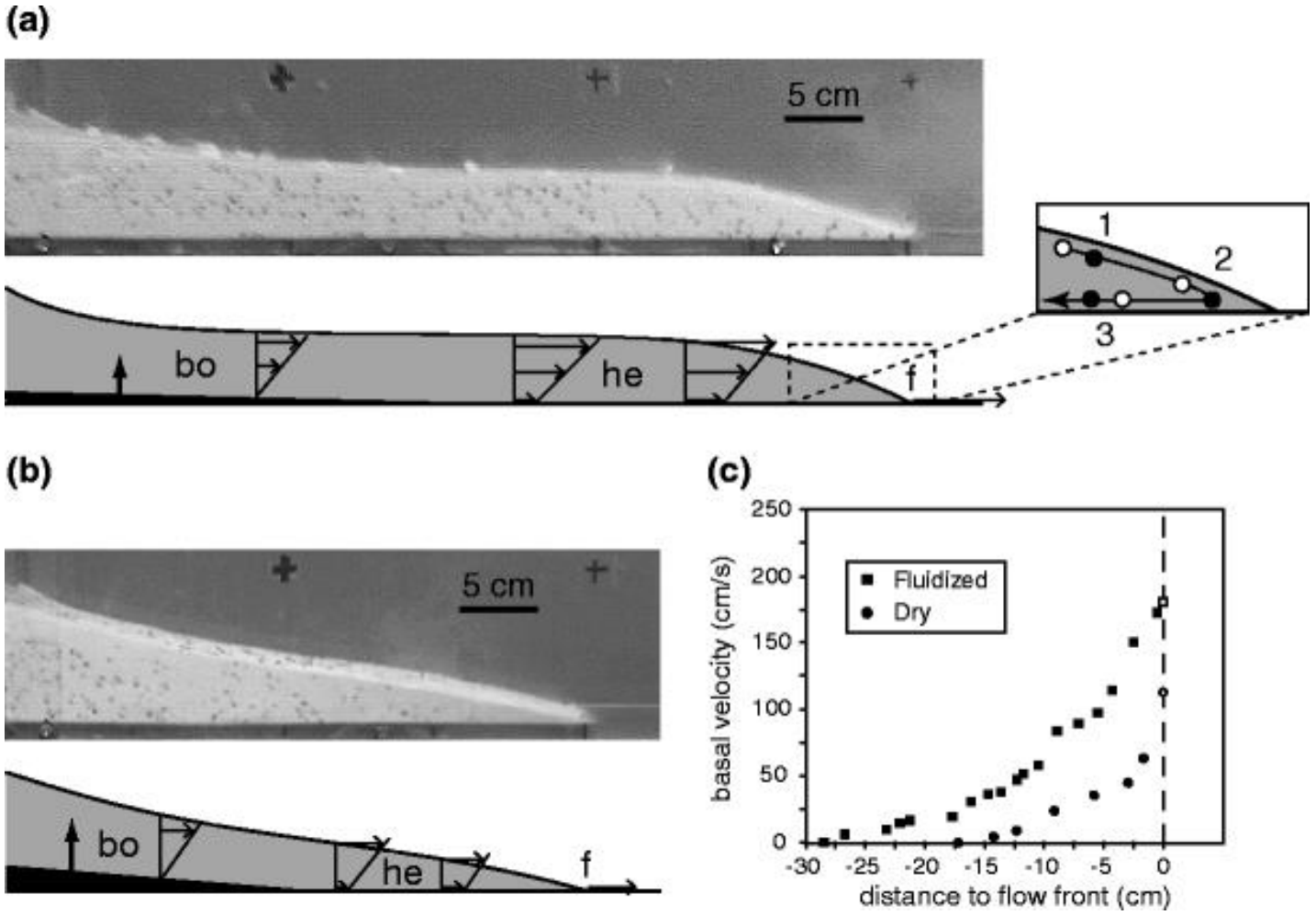

Roche O. 2012. Depositional processes and gas pore pressure in pyroclastic flows: an experimental perspective. Bull. Volcanol. 74, 1807-1820

observations

Seismic signals of PC at Colima volcano (dome collapse occurred on 2015)

- PC front
- PC body
- PC tail

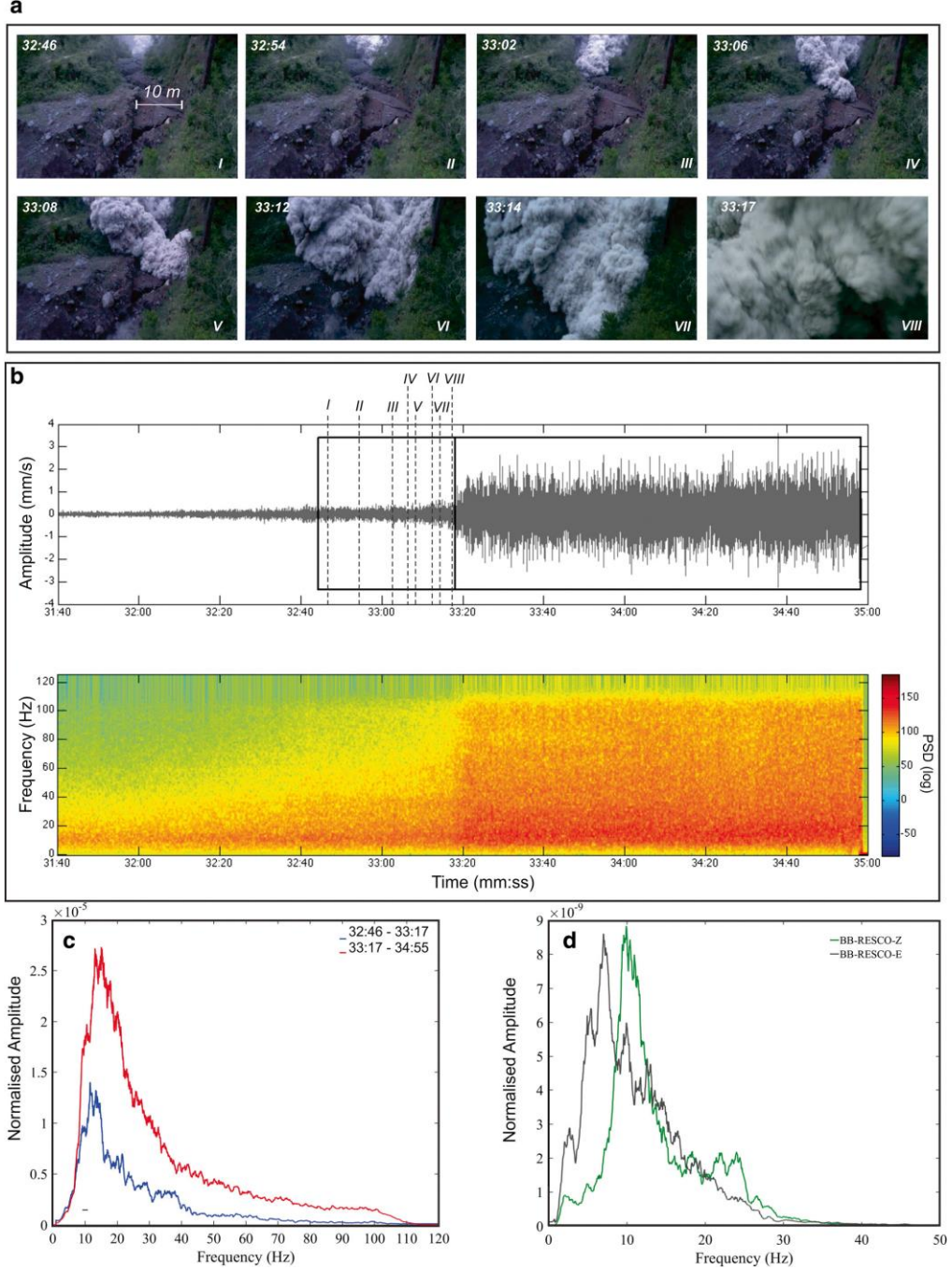

Capra L. et al. 2018. The anatomy of a pyroclastic density current: the 10 July 2015 event at Volcan de Colima (Mexico). Bull. Volcanol. 80, 34

2D numerical simulations on turbulent boundary layer evolution in PCs

Straight topography

Convex-upward topography

Concave-upward topography

Simulations with specific 2D volcano sections allow focusing on details like boundary layer processes and deposition, which are related to each other

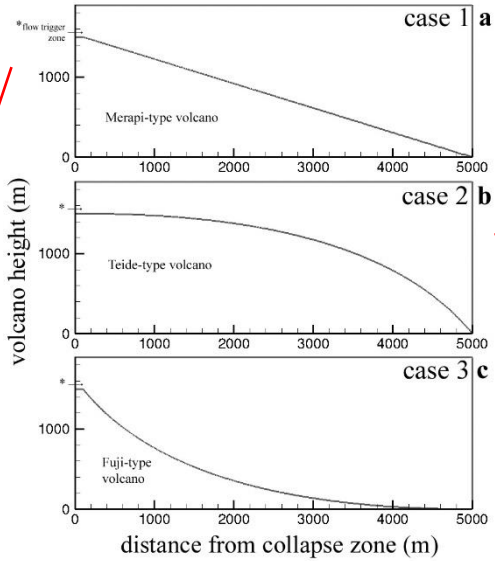

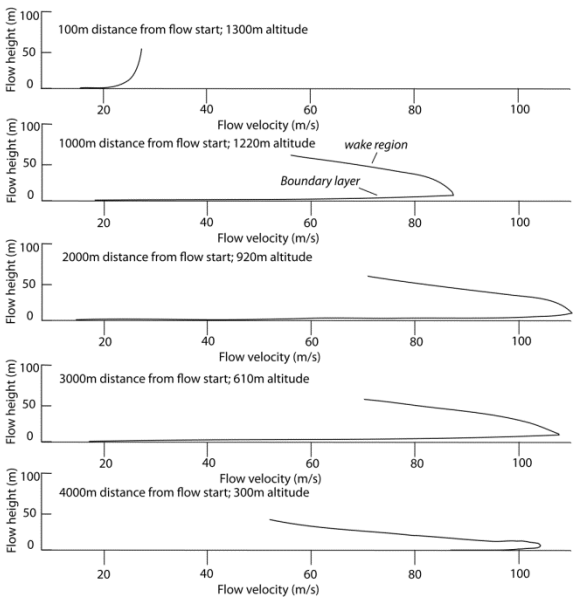

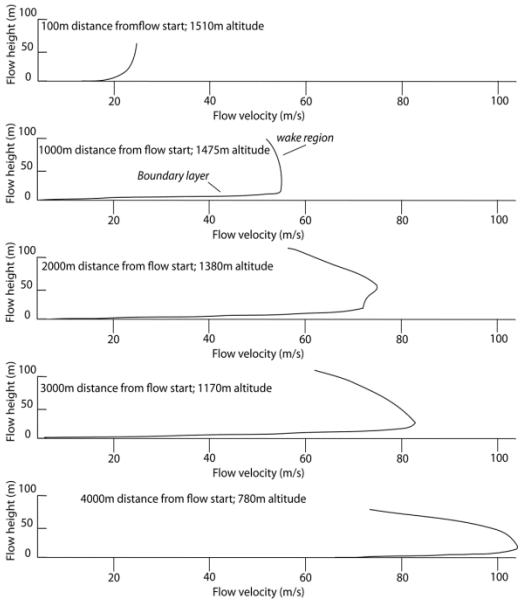

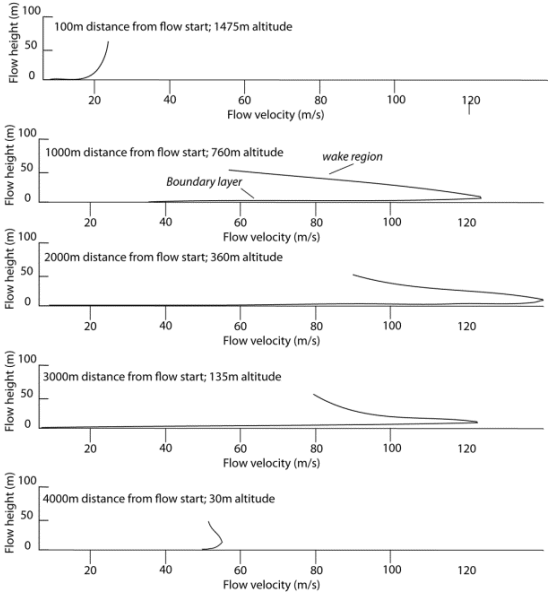

Doronzo D.M., Marti J., Sulpizio R., Dellino P. 2012. Aerodynamics of stratovolcanoes during multiphase processes. J. Geophys. Res. 117, B01207

2D simulations zooming at the scale of deposition, and comparison with field data

The (numerical) grain-size distributions show a poor sorting wherever the boundary layer is not that developed, indicating a low particle selection in the flow, and likely a massive facies in the deposits, whereas they show a better sorting when the boundary layer is more developed, indicating a higher particle selection, and deposits likely having a stratified/laminated facies

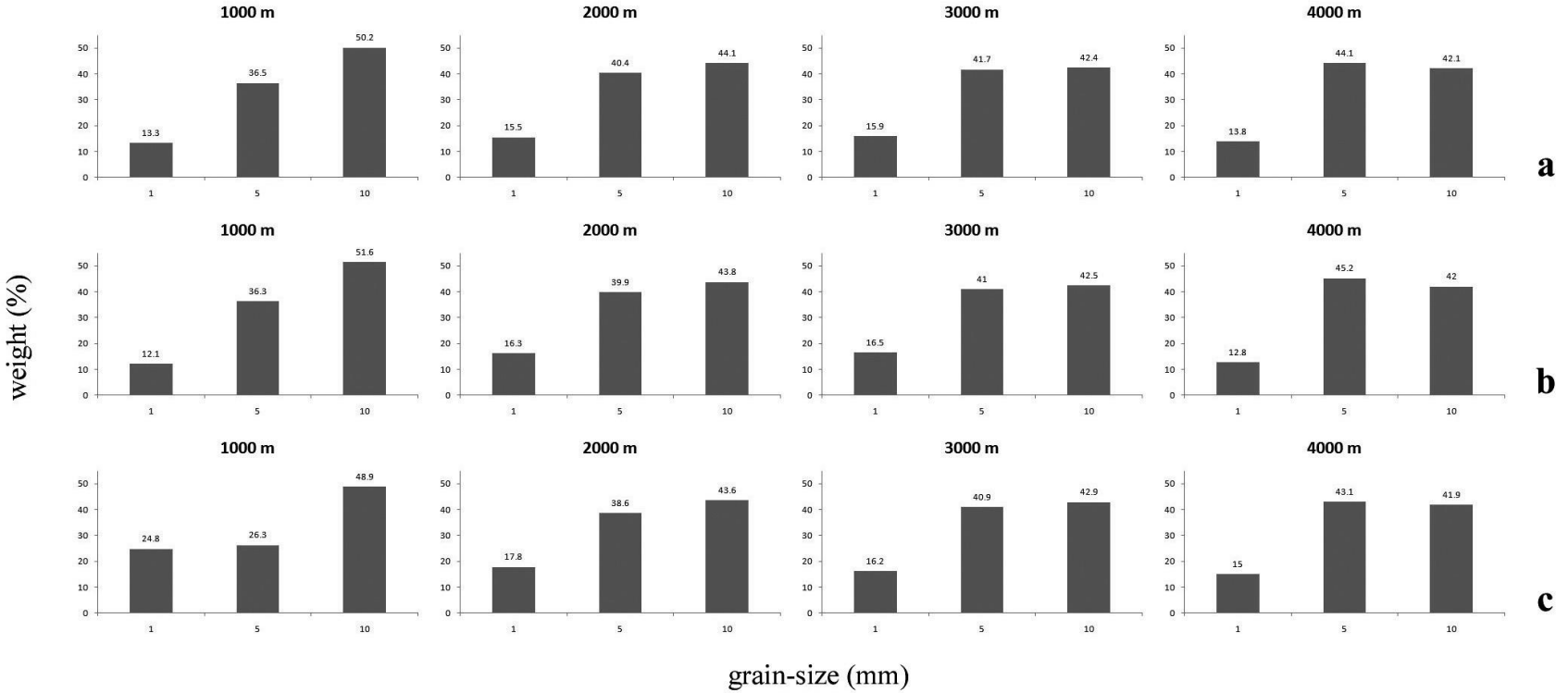

a = straight topography, b = concave-upward topography, c = convex-upward topography

Valentine G.A. et al. 2011. Effects of volcano profile on dilute pyroclastic density currents: Numerical simulations. Geol. 39, 947-950

Numerical simulation for Vulcano Island, and comparison with the field

The numerical model is Eulerian-Lagrangian multiphase-type, solving here also for the energy equation. The computational domain was built using the actual morphology of the island, in order to simulate a pressure-balanced jet collapse, and the propagation of an intermediate volume PC over 3D actual topography

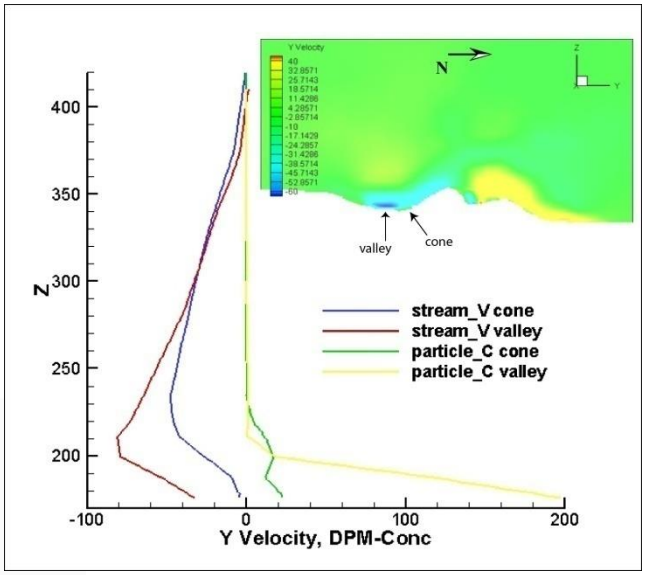

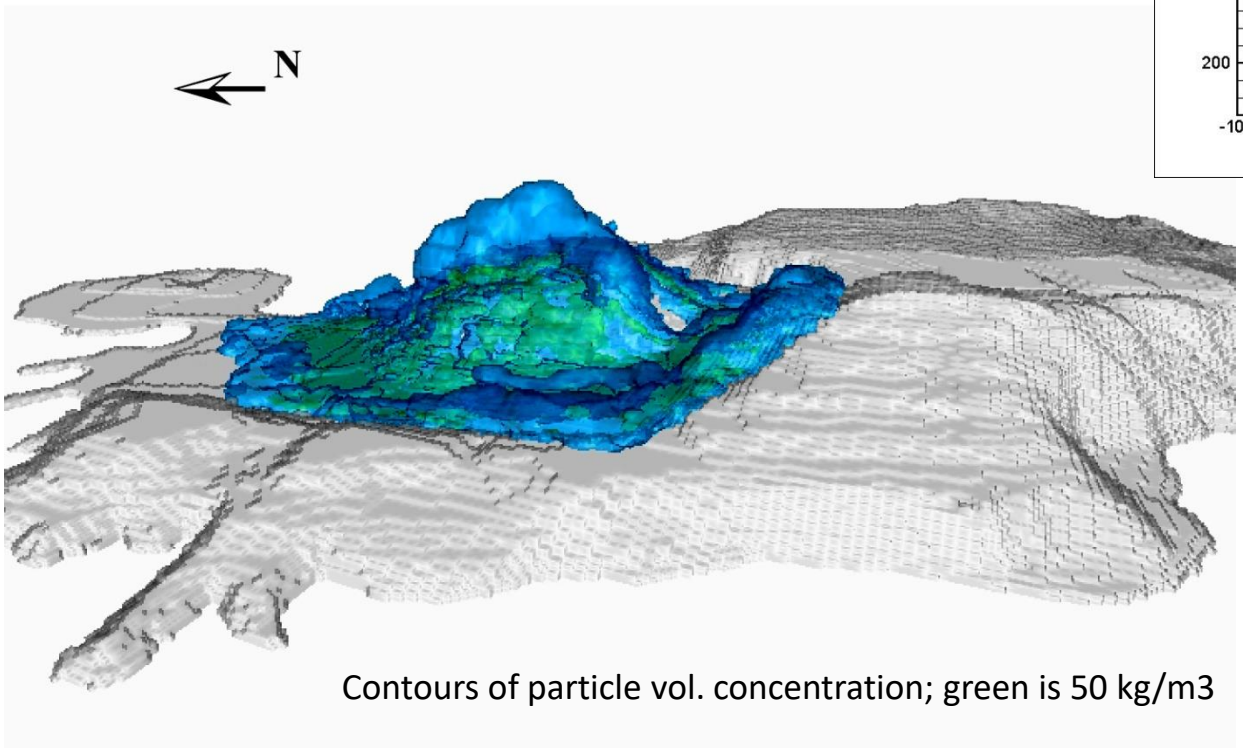

Contours of particle vol. concentration; green is 50 kg/m3

Velocity and particle mass concentration profiles in a North-South section. Contours of PC velocity in the inset. The profiles have a shape similar to those experimentally-observed for particle-laden density currents

Doronzo D.M., Dellino P. 2014. Pyroclastic density currents and local topography as seen with the conveyer model. JVGR 278-279, 25-39

3) DEPOSITION

Application of the numerical model to Vulcano Island, and comparison with the field

Map of PC dynamic pressures

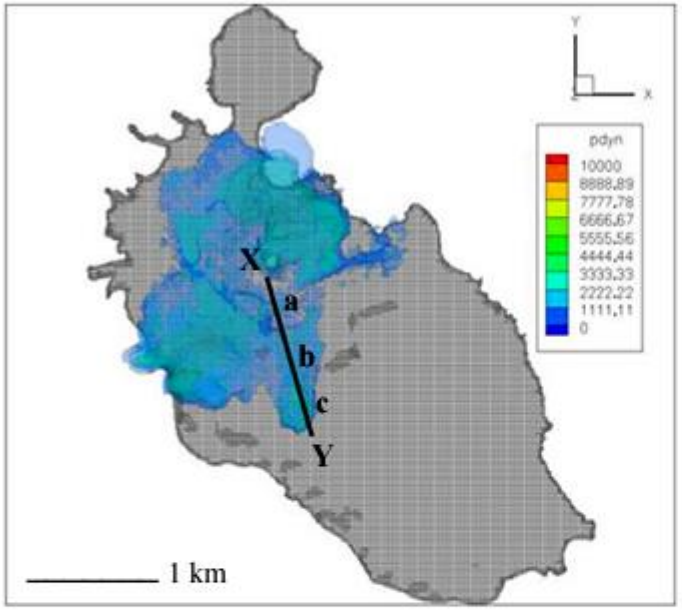

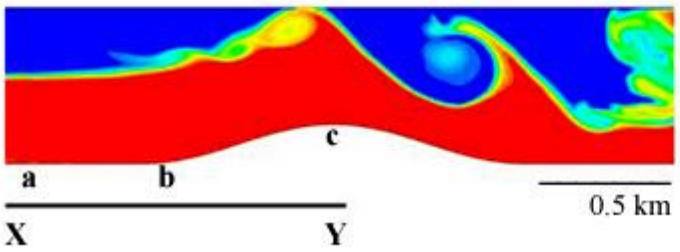

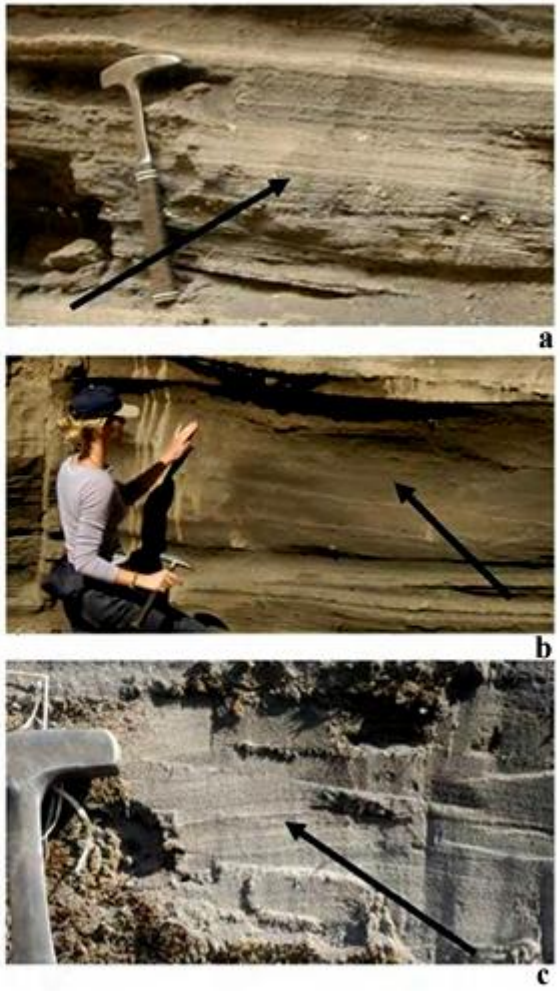

Natural PC deposits with proximal laminated (a), medium massive (b), and distal laminated (c) facies. Such facies reflect the behavior of the sedimentation rate versus deposition rate. The first one depends on particle settling, whereas the second one depends on the ability of the flow to laterally discharge the particles over topography; such ability depends on eruption style, duration, and local topography

Doronzo D.M. et al. 2017. Merging field mapping and numerical simulation to interpret the lithofacies variations from unsteady pyroclastic density currents on uneven terrain: The case of La Fossa di Vulcano (Aeolian Islands, Italy). J. Volcanol. Geotherm. Res. 330, 36-42

Application of the numerical model to Vulcano Island, and comparison with the field

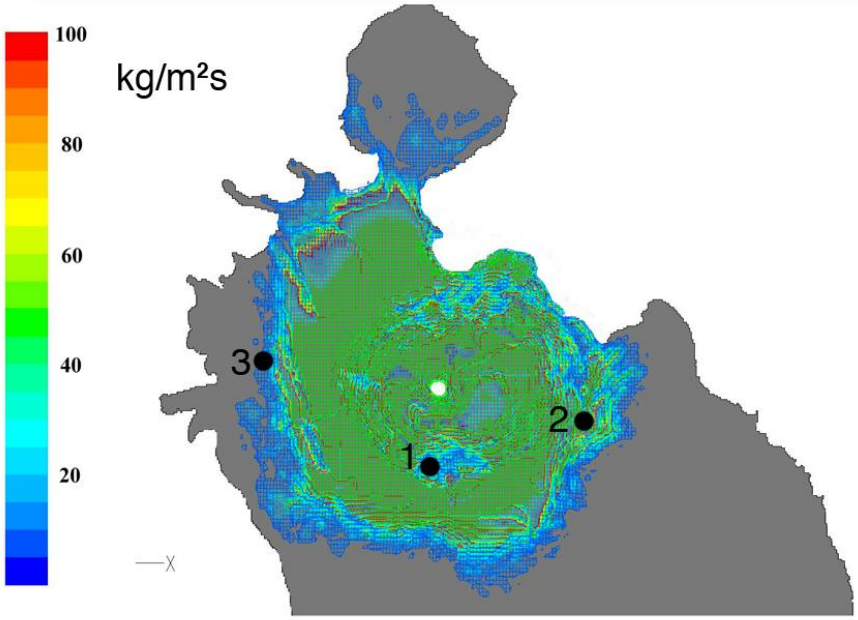

sedimentation rate

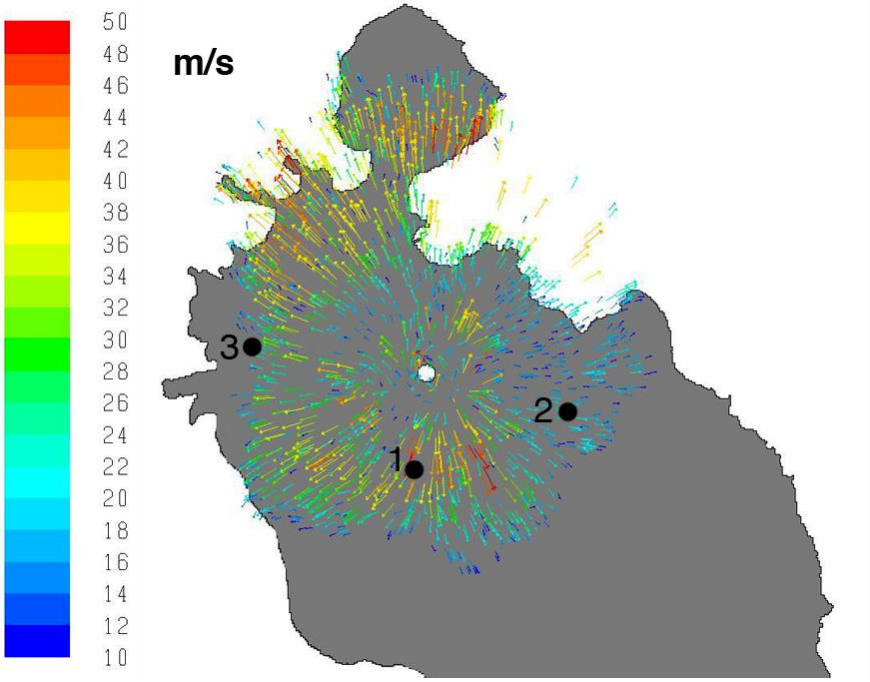

flow velocity

km-scale

Model constraints (componentry, grain-size) from field sedimentology

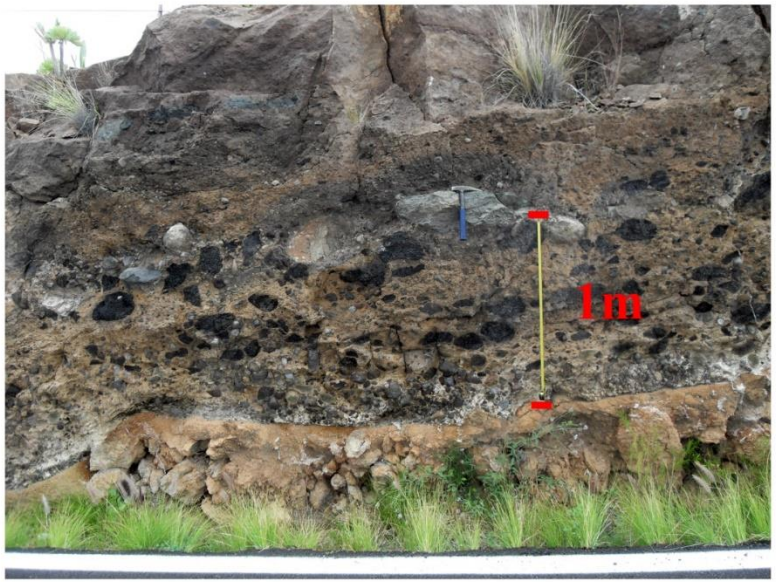

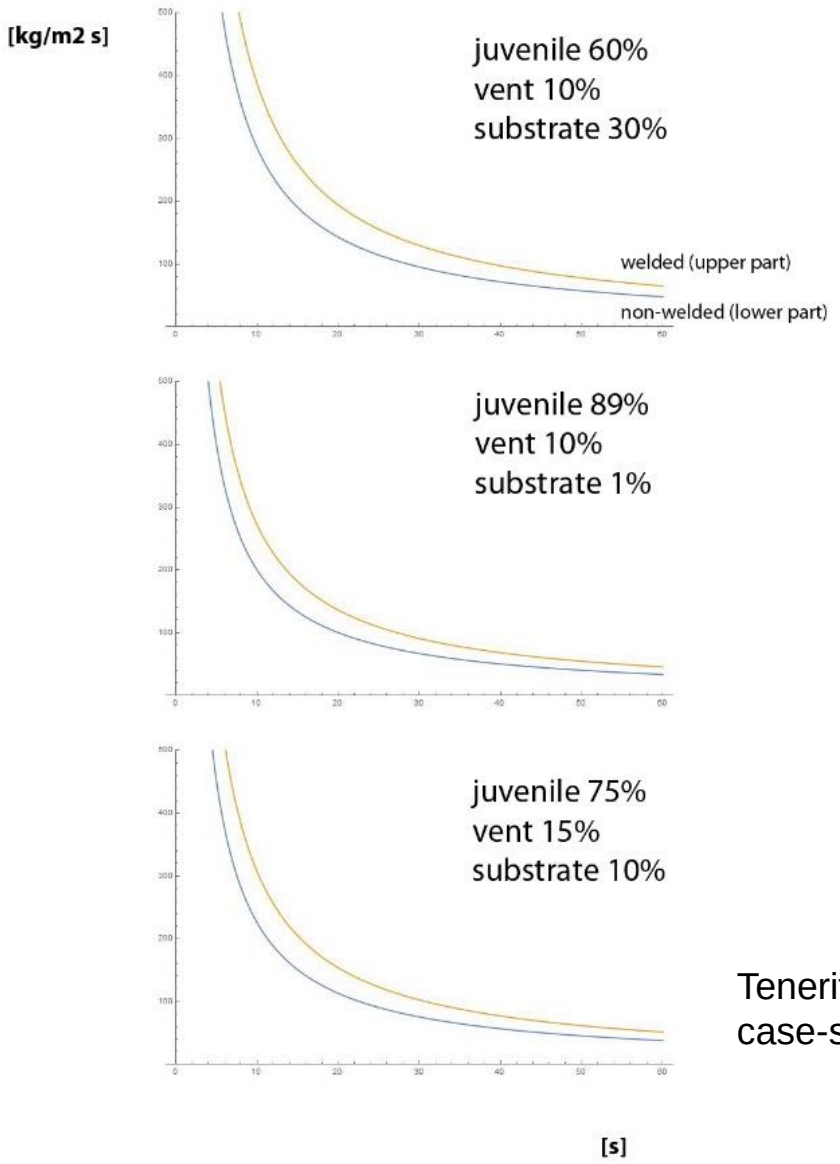

Tenerife case-study

Marti J., Doronzo D.M. et al. 2019. Topographical controls on small-volume pyroclastic flows. Sedimentol. 66, 2297-2317

Local flow properties and emplacement are reflected by local componentry and grain-size; local accumulation rates were calculated for Andean ignimbrites

$$A_r = \frac{T_{empl}}{T_{juv}C_{juv} + T_{obsid}C_{obsid} + T_{lith}\left(1 - C_{juv} - C_{obsid}\right)} \cdot \frac{h_{unit}\,\rho_p}{t_{empl}}$$

Site ID	h [m]	A_r min-max [kg/m² s]	t min-max [min]	h/t min-max [mm/s]					
8	12	0.6 - 11.2	25.0 - 500.0	0.4 - 8.0					
100	23	2.1 - 41.1	13.0 - 260.9	1.5 - 29.4					
102	80	24.9 - 497.8	3.7 - 75.0	17.8 - 355.6					
106	16	1.0 - 19.9	18.7 - 375.0	0.7 - 14.2					
113	6	0.1 - 2.8	50.0 - 1000.0	0.1 - 2.0					
115	50	9.7 - 194.4	6.0 - 120.0	6.9 - 138.9					
125	85	28.1 - 561.9	3.5 - 70.6	20.1 - 401.4					
127	200	155.5 - 3111.1	1.5 - 30.0	111.1 - 2222.2					
133	87	29.4 - 588.7	3.4 - 69.0	21.0 - 420.5					
138	50	9.7 - 194.4	6.0 - 120.0	6.9 - 138.9					
140	51	10.1 - 202.3	5.9 - 117.6	7.2 - 144.5					
148	12	0.6 – 11.2	25.0 – 500.0	0.4 - 8.0					
149	10	0.4 – 7.8	30.0 – 600.0	0.3 - 5.6					
434	141	77.3 - 1546.3	2.1 - 42.5	55.2 - 1104.5					

Coranzulì case-study

Guzman S., Doronzo D.M. et al. 2020. Characteristics and emplacement mechanisms of the Coranzulì ignimbrites (Central Andes). Sed. Geol. 405, 105669

Topographic effects over a hundred meters affect flow deposit thickness through a local accumulation rate

Tenerife case-study

Depositional sequence of the A.D. 79 “Pompei” eruption of Vesuvius: a sequence of processes from magma to tephra

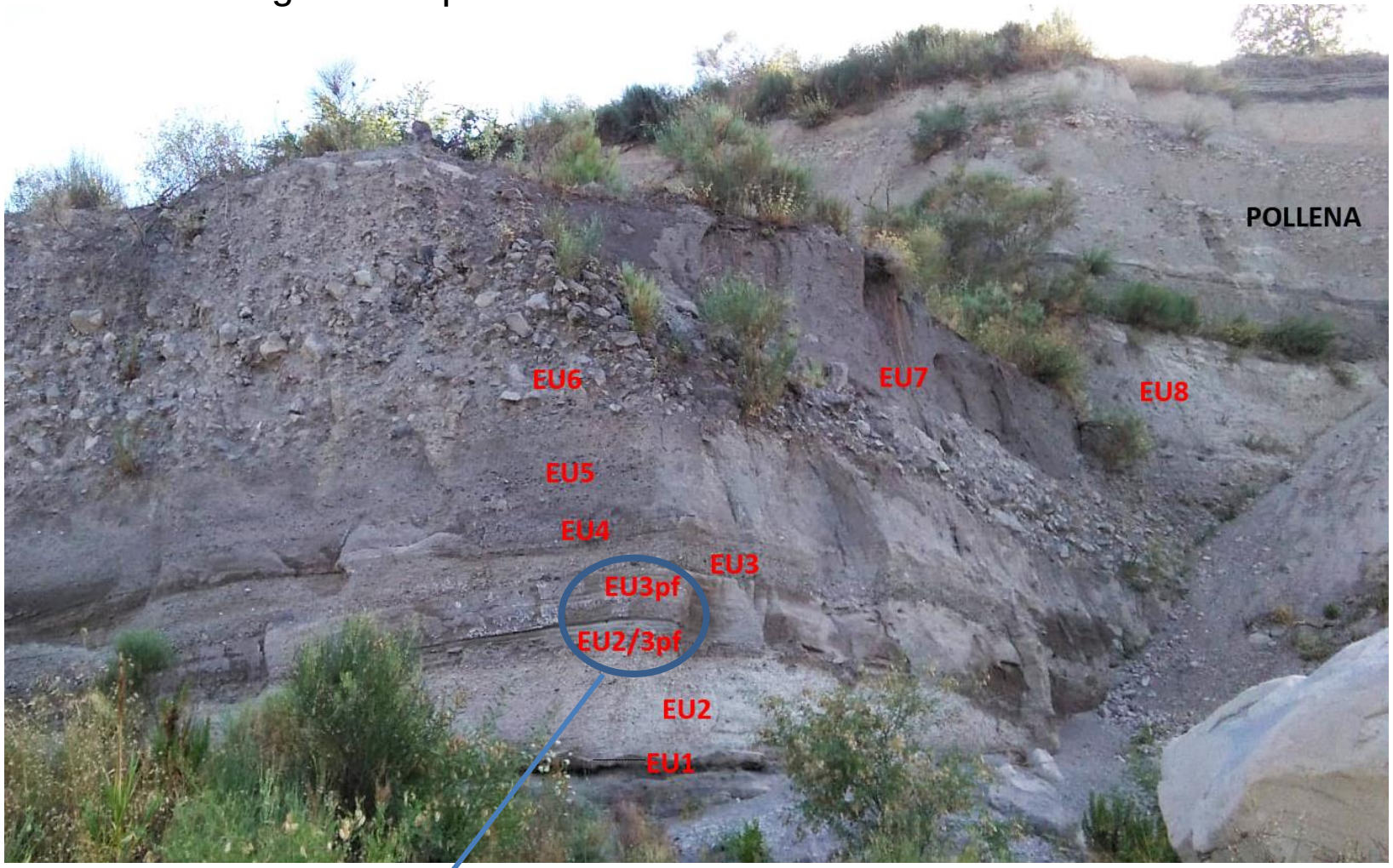

partial collapses can depend on compositional/textural variations in the conduit (e.g., lateral variation of magma density and differential decompression rate)

Shea T., Gurioli L., Houghton B.F. 2012. Transitions between fall phases and pyroclastic density currents during the AD 79 eruption at Vesuvius…. Bull. Volcanol. 74, 2363-2381

Geological map of Vesuvius

local topography, local deposits, etc

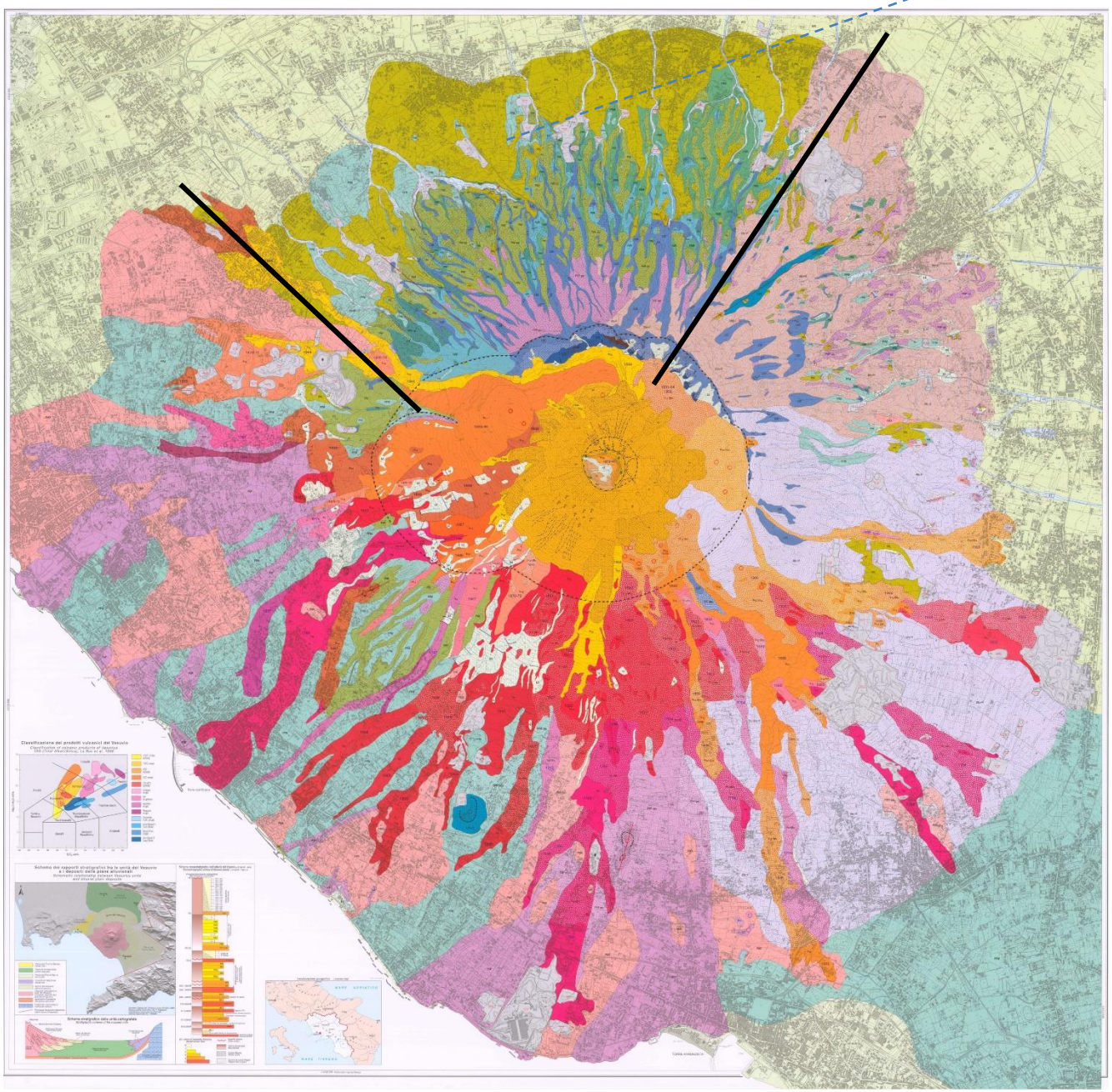

Geological maps are a complete way not only to report the history for example of a volcano, but also to synthesize the sequence of physical processes responsible for field deposits (e.g., eruption unit thickness, grain-size, componentry, geochemistry, paleotemperature)

4) IMPACT (at building scale and from people's side)

Impact of PCs on an isolated building, and comparison with observations

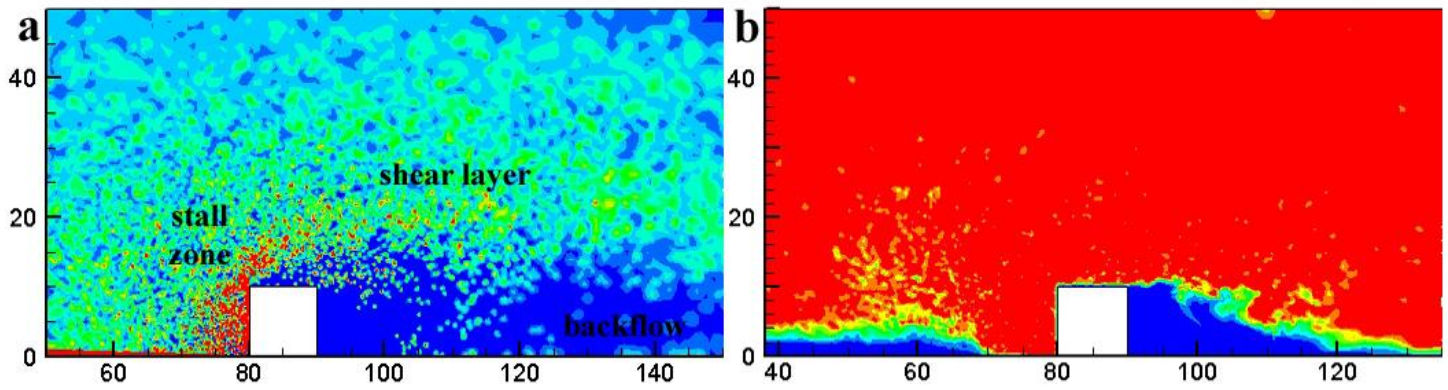

2D simulations of a 50m-thick stratified PC entering left to right, and impacting a 10m x 10m building

Built environments are settings of high particle sedimentation, and flow turbulence because of the loss of equilibrium of the boundary layer

(from Doronzo and Dellino 2011, EPSL)

Experimental PC deposits against scaled buildings

Signals of normalized dynamic pressures (Doronzo 2013, Bull. Volcanol.)

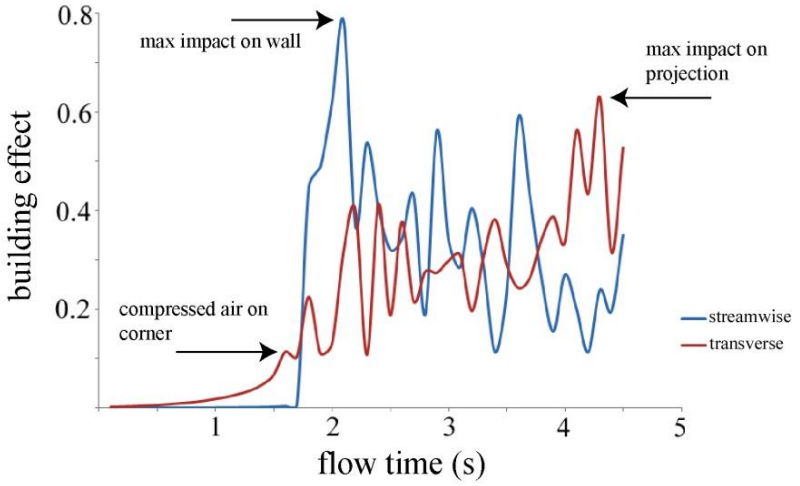

Simulations of PC-building interaction, and comparison with observations

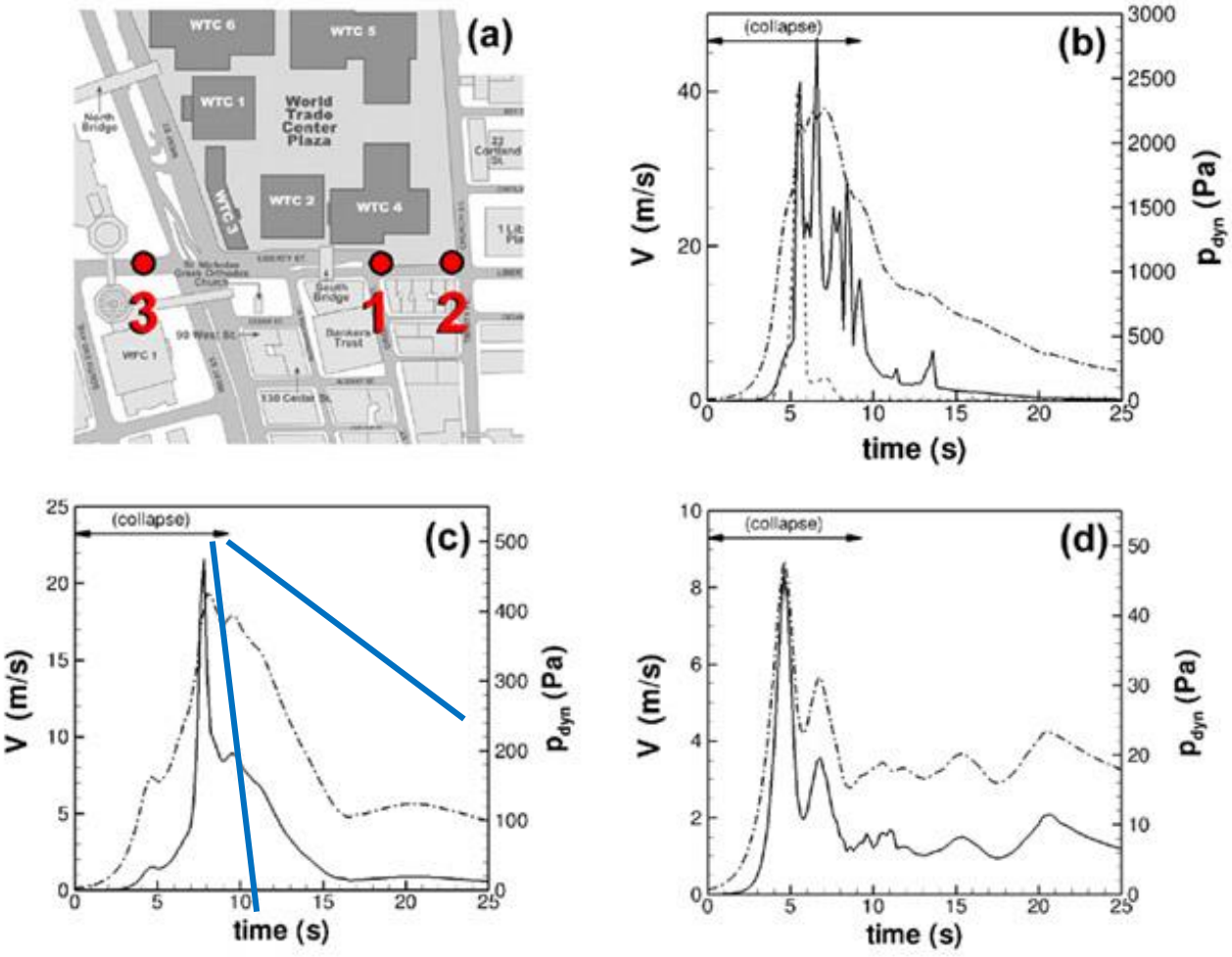

Flow dynamic pressures and velocities of dusty currents impacting multiple buildings (Doronzo et al. 2015, JVGR)

Simulations of PC-building interaction, and comparison with observations

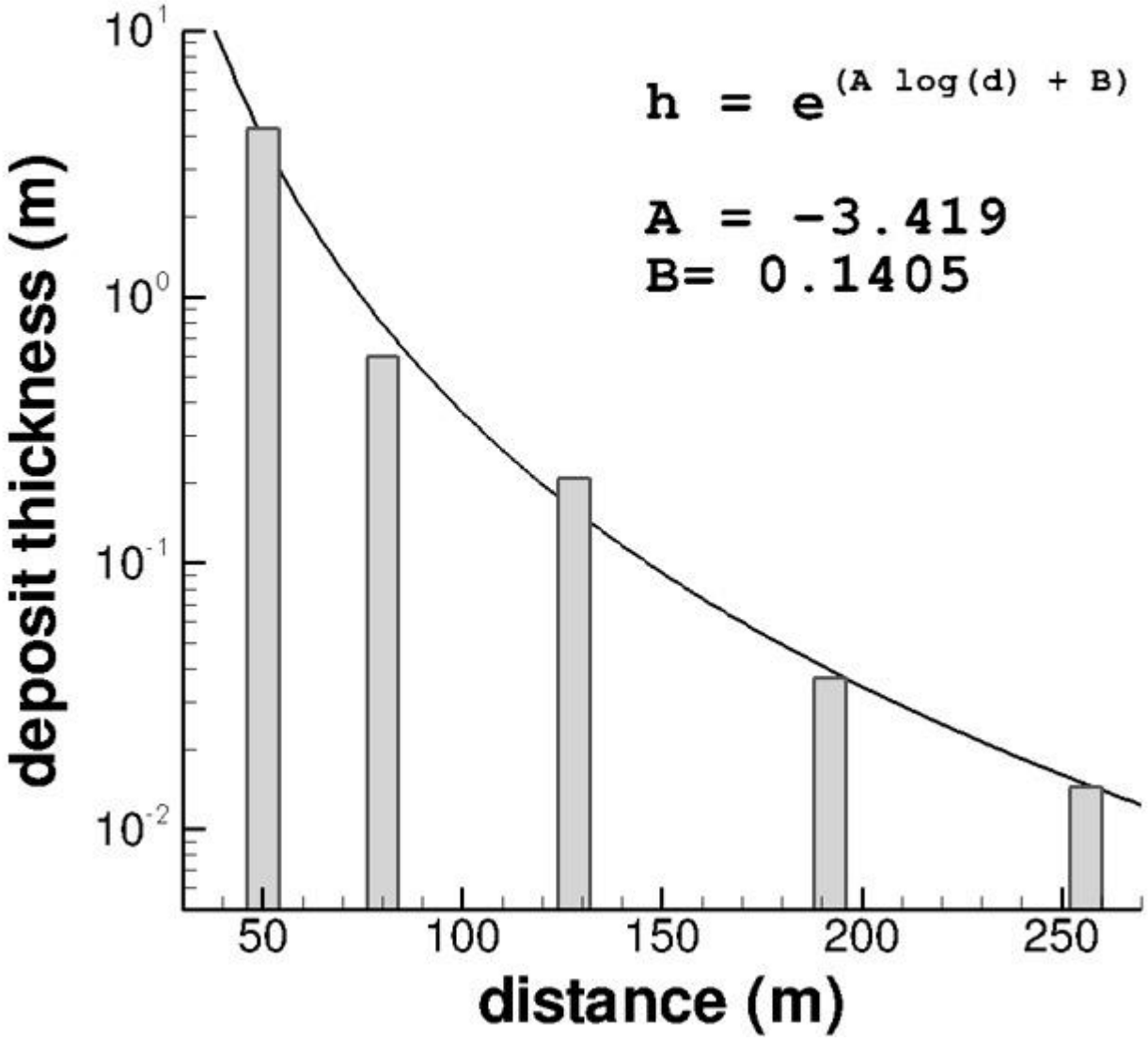

“numerical” deposits from dusty currents after interaction with buildings

Simulations of dust storms in the form of density current using multiphase model

Pulsating case

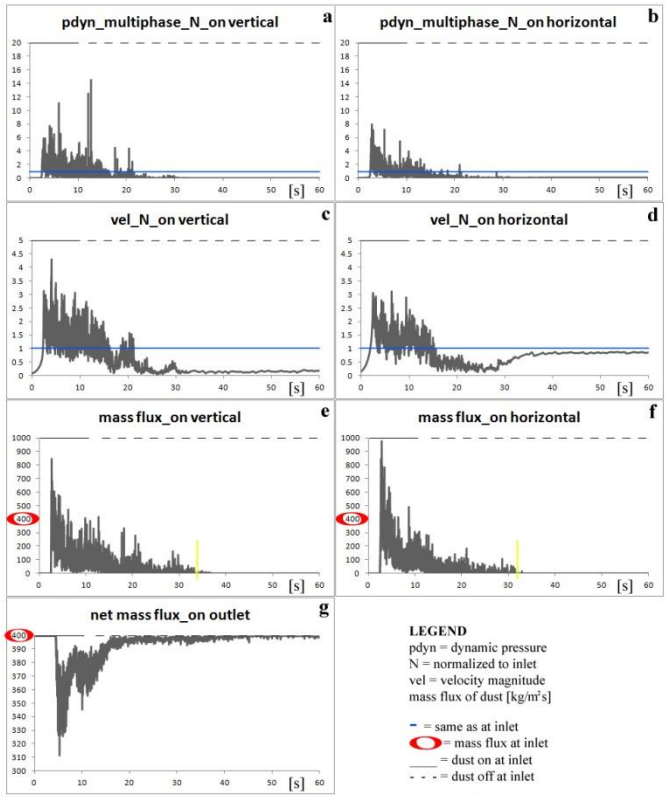

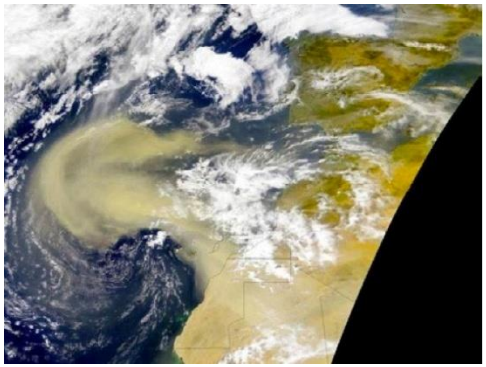

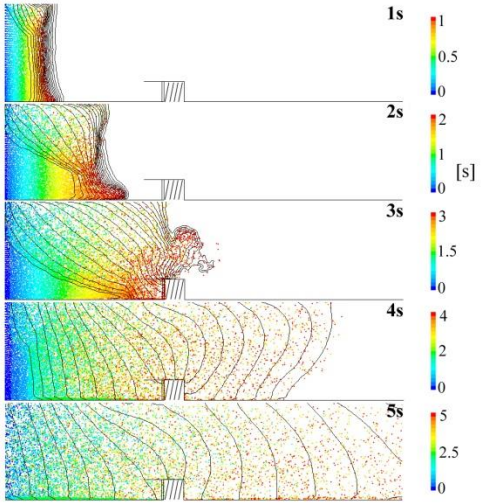

Sustained case

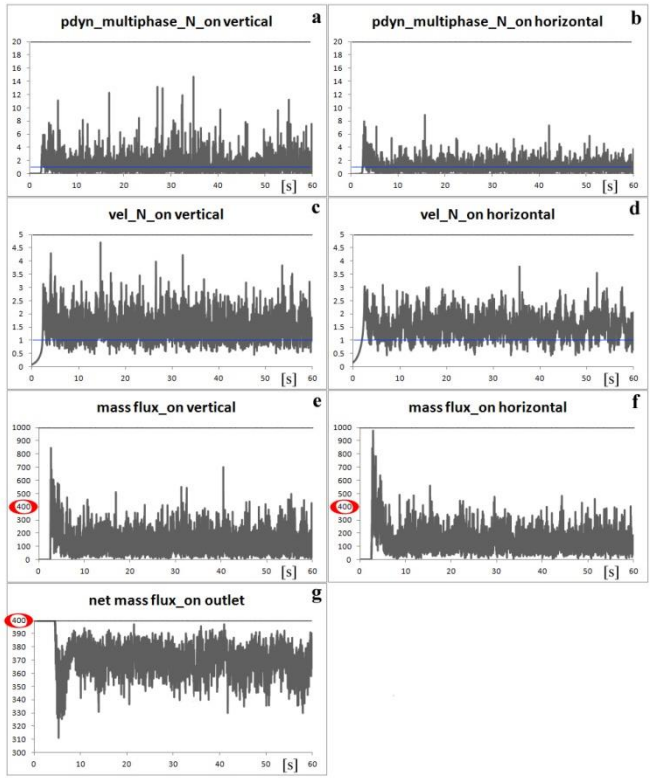

Conclusions

- 3D numerical **multiphase**-flow model can be applied to natural scenarios of eruptions giving PCs

- They have been successfully applied to Vulcano Island, Soufrière, and Mount St. Helens

- More detailed depositional features of PCs can be macroscopically reconstructed with 2D zoomed simulations, always with the fundamental help of **stratigraphy**, sedimentology, and petrology

- Applications to 2D and 3D cases of **PC-building interaction** are useful to assess the hazard at building scale (real perception of hazard from people)

- Multidisciplinary approaches from magma to tephra are necessary for a global view of PCs from vent to deposit

Thanks for your attention

domenico.doronzo@ingv.it